Analysis and modeling of infrasound from a four-stage rocket launch

Philip Blom,[1,a)] Omar Marcillo,[1] and Stephen Arrowsmith[2]
[1]*Los Alamos National Laboratory, Los Alamos, New Mexico 87545, USA*
[2]*Sandia National Laboratory, Albuquerque, New Mexico 87321, USA*

Infrasound from a four-stage sounding rocket was recorded by several arrays within 100 km of the launch pad. Propagation modeling methods have been applied to the known trajectory to predict infrasonic signals at the ground in order to identify what information might be obtained from such observations. There is good agreement between modeled and observed back azimuths, and predicted arrival times for motor ignition signals match those observed. The signal due to the high-altitude stage ignition is found to be low amplitude, despite predictions of weak attenuation. This lack of signal is possibly due to inefficient aeroacoustic coupling in the rarefied upper atmosphere. © 2016 Acoustical Society of America. [http://dx.doi.org/10.1121/1.4953817]

[VEO]   Pages: 3134–3138

I. INTRODUCTION

Infrasound is of particular interest for the remote monitoring of energetic natural and anthropogenic sources in the atmosphere because it propagates long distances without significant attenuation. Previous studies on the measurement of infrasound generated by rockets have primarily been restricted to long-range observations of launches,[1–4] or to static motor tests at shorter range.[5,6] The main sources of infrasound due to rockets are aeroacoustic energy produced by supersonic engine exhaust gases and, in the case of a launch, the Mach cone formed when the rocket reaches supersonic velocities.[5,7] At short ranges for static motor tests, the duration of infrasound correlates to burn time, amplitude to motor thrust, and frequency content to a variety of effects including exhaust velocity, thrust, and type of rocket motor.[5,6] At long range the distortion of signals by atmospheric propagation makes interpretation more complex, although correlations between sound intensity and vehicle size have been observed, as have differences in signal characteristics with motor type.[8]

This study focuses on the analysis of infrasound from a multi-stage sounding rocket launch observed at several infrasound arrays located between 7 and 100 km from the launch pad. At such close distances, only the infrasound produced by the motor exhaust is expected to be observed, as the Mach cone does not form until the rocket is aloft and the related energy is primarily directed upward.[7,9] The signals from the Mach cone may be observed as stratospheric and thermospheric returns, but such arrivals are beyond the 100 km range of the arrays included in this study. The only previous analysis of infrasound from a multi-stage sounding rocket in the literature focused primarily on correlating spectral features of recorded infrasound to rocket motor characteristics.[8] A detailed comparison between the observation and modeling of a ground-truth rocket launch with known trajectory and altitudes of rocket motor ignitions and burnouts allows us to assess whether duration can be related to burn time for a moving rocket, determine how well the modeled arrival times and back azimuths correlate with observations for a moving source, and identify what information might be retrieved about the source using such observations and how the quality of this information varies with standoff range.

II. ROCKET LAUNCH AND DATA ANALYSIS

At 08:05:00 UTC on November 24, 2014, a four-stage Talos-Terrier-Brant-Nihka (Black Brant XII) rocket was launched from the Andøya Space Center in Norway toward the northwest as shown in Fig. 1. Ground truth information provided to the researchers included the trajectory of the rocket obtained via GPS positioning and the nominal times and altitudes of the stage ignitions and burnouts, apogee, and impact as summarized in Table I. The ignition locations along the trajectory are indicated by the stars in Fig. 1. Infrasound from the rocket was detected at three arrays at distances of 7.1, 49.0, and 104.8 km from the launch pad during the launch burns. The SKD and BUK arrays were deployed as part of the Norway Stratosphere Experiment (NORSE) experiment[10] and consist of four Hyperion IFS-3010 microbarometers, although the BUK array only contained three sensors at the time of the rocket launch. I37 is an International Monitoring System (IMS) infrasound array operated as part of the Comprehensive Nuclear Test Ban Treaty Organization monitoring network, which contains 9 MB 2005 microbarometers. The Hyperion sensors have a flat response from 0.02 to 200 Hz and the MB 2005 sensors have flat response from 0.01 to 20 Hz. Wind noise reduction is achieved via mechanical filtering using porous hoses at NORSE stations and pipe arrays at the IMS station.[11] The wind noise reduction methods limit the frequency band to below approximately 10 Hz.

The infrasonic signals observed on these three arrays have been analyzed using a frequency range of 2–10 Hz and the results are detailed in Fig. 2. At SKD, three discrete
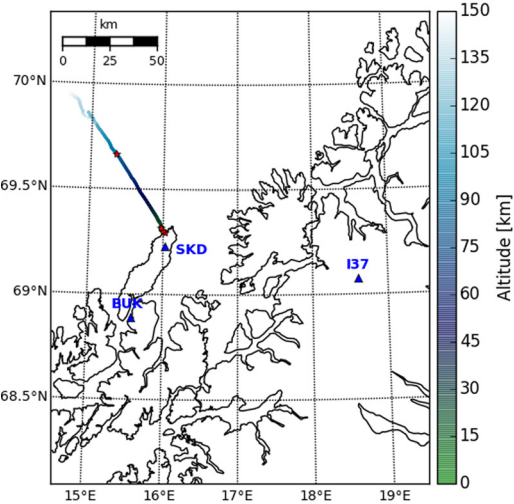
a)Electronic mail: pblom@lanl.gov

FIG. 1. (Color online) The three arrays used in this study (triangles), the trajectory of the rocket path during the motor burns (line), and the locations of the stage ignitions (stars) as detailed in Table I.

infrasound arrival packets were observed within 250 s of the launch and a low amplitude transient signal was observed at approximately 450 s. The spectral content of the various stages shifts to lower frequency with increased time. Each arrival packet has a sharp initial onset, a known characteristic of solid rocket motors,[8] followed by a period of enhanced power that slowly tapers off as the motor burns. In some cases, additional peaks are observed within a given arrival packet. The spectral content is dominantly above 1 Hz, with high frequency content up to the Nyquist (100 Hz) for the first two packets and less energy at high frequency for the later two packets. At BUK, the signal-to-noise ratio was poor, but it is possible to discern a short duration signal at approximately 125 s followed by a long packet of energy between 250 and 350 s. At I37, two distinct phases were observed separated by roughly 150 s. The signal just after 300 s is a short transient, but the later signal has longer duration and variable amplitude. The sharp onsets at SKD are less pronounced or not present at BUK and I37.

III. MODELING THE INFRASOUND OBSERVATIONS

Using the ground-truth trajectory, the infrasound propagation times and back azimuths at each array has been

TABLE I. Altitudes and flight times of motor ignitions and burnouts for the Talos-Terrier-Brant-Nihka rocket motor stages as well as apogee and impact.

Event	Alt (km)	Flight (s)
Talos Ignition	0.1	0.0
Talos Burnout	1.8	6.4
Terrier Ignition	7.8	25.0
Terrier Burnout	10.6	31.2
Black Brant Ignition	14.4	37.0
Black Brant Burnout	55.0	71.0
Nihka Ignition	95.0	94.0
Nihka Burnout	143.5	117.0
Apogee	529.7	422.3
Impact	0.0	781.2

predicted using the ray tracing methods developed by Blom and Waxler[12] extended to model propagation in a three dimensional, inhomogeneous, moving medium with a coordinate transformation to model propagation in an atmosphere layer surrounding a spherical globe. In this case, horizontal propagation distances are limited to 100–200 km and range dependence in the atmosphere can be ignored. Propagation modeling analysis utilized a Levenberg-Marquardt method for identifying eigenrays (paths connecting a specified source and receiver) that exploits the auxiliary parameters used to calculate geometric spreading along rays. The details of this method are planned to be published in the near future. For discrete heights along the rocket trajectory, eigenrays have been identified which connect the source and receiver within a miss distance of 10 m. It is unlikely that energy is present along all eigenrays as signal is generated only when the motors are burning; however, for the sake of brevity, we will consider eigenrays along the entire trajectory.

Propagation modeling utilized the atmosphere specification for the launch pad location at 08:00 UTC on the date of the launch as obtained from the Ground-to-Space (G2S) database.[13] The adiabatic sound speed and wind fields for the specification are shown in Figs. 3(a) and 3(b). It should be noted that sub-grid scale variations (such as gravity waves) are not included in the G2S specification. Therefore, additional considerations must be made in a more detailed analysis of the propagation as uncertainties in the propagation medium will likely be the dominant source of uncertainties in the estimated trajectory and motor characterization. For the preliminary analysis here, the G2S specifications has been used without such perturbations.

Comparison between the observed and predicted arrival times and back azimuths for each array are included in Fig. 2, where the blue points denote the predicted values and the black points denote those observed. At SKD, the predicted arrival times and recorded durations of discrete rocket stages fit the observations closely with the higher amplitude onset signals correlating well with the estimated onsets for the three lower altitude stages (denoted as the dashed lines in the time series). A discrepancy at roughly 100 s is likely associated with an error in the ground-truth GPS data, as it corresponds to a sudden, short duration change in the rocket's horizontal motion to velocities on the order of 2000 km/s. The high altitude ignition of the Nihka rocket was detected with very low amplitude and energy dominantly below 5 Hz.

The trace velocities predictions at SKD are in agreement with observations for the initial 90–100 s of the observed signal; however, there is a consistent bias in the later portion of the trajectory. This difference begins coincident with the back azimuth discrepancy mentioned previously and is likely due to errors in the ground-truth trajectory. It is also worth noting that for faster trace velocities, such as those in the later portion of the trajectory, a difference of 100 m/s in trace velocity corresponds to an arrival inclination difference of approximately 5°. The frequency content of the signals recorded at SKD decrease with time, which is partially explained by the Doppler shift associated with the change in velocity of the rocket as it moves away from the receiver array. In addition to the Doppler shift, the low-frequency observations of the Nihka

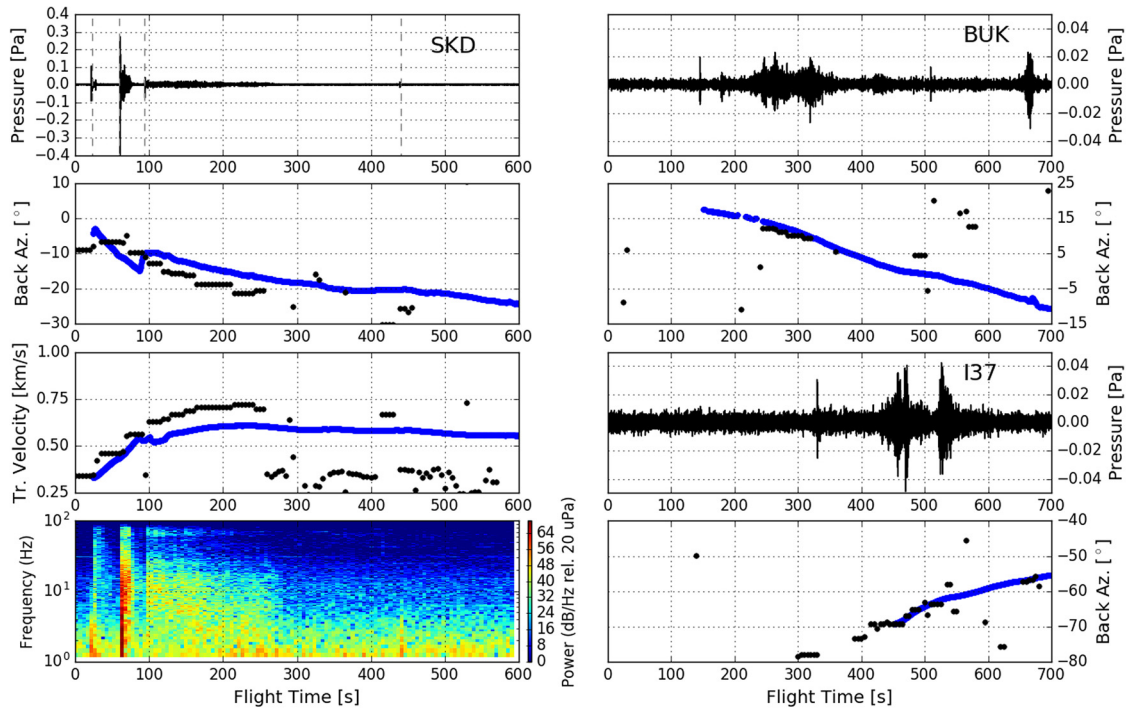J. Acoust. Soc. Am. **139** (6), June 2016

Blom *et al.* 3135

FIG. 2. (Color online) Results of analysis for the infrasonic signals generated by the rocket launch as observed at the arrays used in this study. The observed back azimuth and trace velocities (black) are compared with those predicted using eigenray analysis along the rocket trajectory as provided by the GPS tracking (blue). The vertical dashed lines on the SKD time series denote the predicted arrival times of the motor ignition signals.

ignition are possibly due to the absorption of high-frequency energy in the upper atmosphere.[14]

The eigenray analysis predicts that BUK and I37 will only observe the rocket along the portion of the trajectory for which the altitude is above 7 and 37 km, respectively. The Black Brant burnout and Nihka ignition and burnout are predicted to be observable at I37 and the full ignition and burn out of the Terrier, Black Brant, and Nihka stages are expected to be observed at BUK. The back azimuths and arrival times of the signals observed are in agreement with observations. Because of the increased propagation distance, there are higher uncertainties in the predictions at these locations. The transient signal at BUK is likely due to the Terrier stage ignition, but is found to be less coherent and not well detected. The later signal around 300 s is likely the Black Brant motor burn. At I37, the early transient arrival is not predicted by ray

tracing methods but is possibly the Black Brant ignition arriving due to inaccuracies in the atmospheric specifications or via non-geometric propagation (i.e., scattering or diffraction). The later signal is likely the continued burn of the Brant motor once the rocket reaches 37 km altitude.

In addition to computing eigenrays to model the expected signal at the array locations, the ensonification has been computed for the airborne stage ignitions to determine the "footprint" of the high energy infrasonic transients produced by the ignitions. The resulting arrivals are shown in Fig. 3(d)–3(f). The amplitudes in the figure are relative to 1 km from the source and include geometric spreading effects, variations in density and sound speed, and absorption as specified by Sutherland and Bass.[14] The high amplitude prediction of the Nihka stage is due to the large difference in density between the source altitude and ground and the
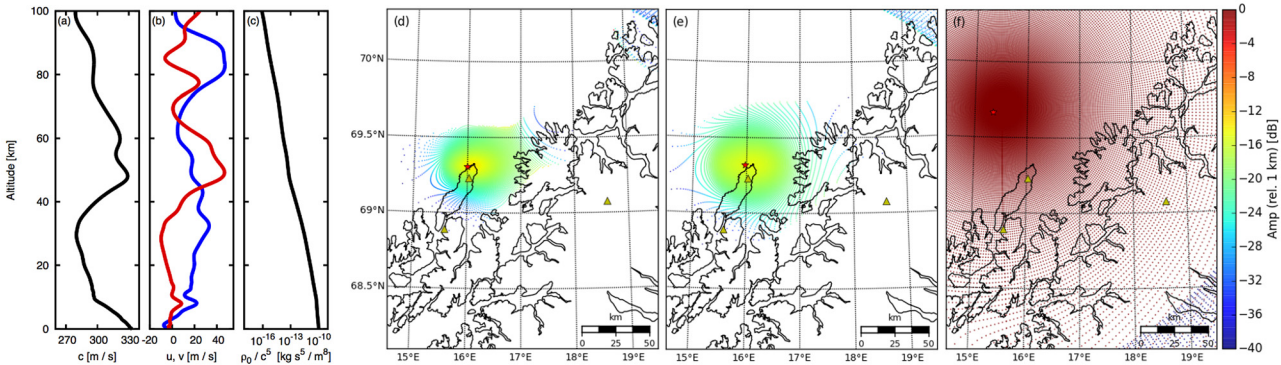

FIG. 3. (Color online) (a–c) Atmospheric specifications for the time and location of the rocket launch acquired from the G2S. (d–f) The predicted ensonification for the airborne motor ignitions of the (d) Terrier (7.8 km altitude), (e) Brant (14.4 km altitude), and (f) Nihka (95.0 km altitude) stages. The weak attenuation of the Nihka stage is due to conservation of energy and the large difference in density at the source altitude and ground.

conservation of energy condition on the amplitude. As determined by the eigenray analysis, SKD is expected to be in the ensonified region for all of the stages, BUK is expected to be near the edge of the ensonified region for all three airborne stages, and I37 is expected to detect the Brant burnout and Nihka ignition and burnout. Despite the large ensonified region and weak attenuation predicted for the Nihka stage, only SKD detected a signal with an arrival time consistent with the stage and the motor burn produced no observed signals. The lack of such observations is possibly due to the lower power of the aeroacoustic source in the rarefied upper atmosphere. The total acoustic power produced by an aerodynamic source, such as rocket exhaust, can be shown to be proportional to,[15]

$$\mathcal{P}_{ac} \propto \frac{\rho_0}{c_0{}^5} U^8 l^2, \qquad (1)$$

where ρ_0 is the density of the ambient fluid, c_0 is the sound speed outside of the flow, U is the flow velocity, and l is the linear dimension of the flow. In this case, the value of $\rho_0/c_0{}^5$ varies with altitude as shown in Fig. 3(c). From the value of this ratio, rocket motors with comparable exhaust characteristics will produce aeroacoustic power at an altitude of 90 km with power approximately 10^{-6} of the same motor near the ground. This altitude dependence provides a possible explanation for the lack of observations corresponding to the Nihka stage of the rocket, as the exhaust from the motor simply did not produce significant acoustic power in the rarefied upper atmosphere.

IV. IMPLICATIONS FOR ROCKET MOTOR CHARACTERIZATION

It is of interest to consider what information one might obtain about a rocket launch if presented only with a set of infrasound measurements such as those in this paper. Of particular interest for reconstruction purposes are details such as the rocket trajectory, the number of stages, and the characteristics of the rocket motors. The most relevant features of the recorded infrasound signals are the duration of arrivals, the frequency content, and the direction-of-arrival (i.e., back azimuth and trace velocity). Our findings clearly demonstrate that significantly more information can be gleaned if one has observations from a location that is sufficiently close to a rocket launch pad to ensure direct eigenrays exist along the entire rocket trajectory. Arrays at larger distances from the launch pad introduce larger propagation effects into the analysis, which can lead to large uncertainties in the infrasonic source and decrease the ability to estimate the trajectory and distinguish stage burns.

On the basis of the analyses in this paper, the following observations can be made regarding the estimation of rocket motor characteristics from infrasonic observations. First, in order to estimate the rocket trajectory, one must have infrasound observations at multiple arrays for that portion of the rocket launch. In this study, this is only possible for altitudes above 7 km due to the distance between the launch pad and BUK. Accurate measurement of the trace velocity for arrays near the launch pad or along the trajectory are also required to estimate the vertical motion of the rocket. Unfortunately, the small numbers of elements at SKD and BUK make such

analysis difficult for this data set and the observed trace velocities observed here exhibit a bias which is possibly due to an error in the ground-truth trajectory. Second, it is necessary to sample the full trajectory in order to identify the number of motor stages. However, due to the rarefaction in the upper atmosphere, the aeroacoustic source mechanism loses efficiency as the rocket increases in altitude and stages fired at high altitude may not be observable due to decreased source power. Finally, to obtain the types of rocket motor, two parameters are most useful: the duration of the recorded signals and the frequency content. From the analysis here, identification of the motor burn durations appears to be feasible if one has the known, or estimated, trajectory. Additionally, the observed spectral characteristics can be converted to a stationary reference frame by correcting for the Doppler shift, providing more information on rocket type.[8]

In this study, only the observations at SKD provide quality information to estimate the number of stages and motor type (impulsive onsets typical of solid rocket motors, observed Doppler shift, and durations that can be retrieved assuming a prior on the launch trajectory). However, the additional information obtained from signals at BUK and I37 allow one to estimate the rocket trajectory so that further analysis is possible using the signals at SKD. A more rigorous analysis might require the application of a full-wave propagation scheme to better identify the ensonified regions by accounting for scattering and diffraction effects. Additionally, analysis could be performed incorporating the appropriate Doppler shift effects to estimate the source spectra from the observed signal spectra. Such a study is beyond the scope of the discussion here, but it is a possible path forward in continued analysis of this data set.

V. CONCLUSIONS

The observations and associated modeling presented here provide some bounds on the type of information that can be obtained from infrasound generated by rockets in addition to constraints on how the information content is affected by standoff range. We conclude that a single array within 20 km of a launch site can provide information on the number of motor stages, motor durations (from retrieved durations, assuming one has prior information on trajectory), and information on velocity (from the observed Doppler shift). Arrays between 20 and 100–200 km sample higher elevations of the trajectory, providing some information regarding higher altitude motor stages; however, the interpretation of these data is much more complex and has not been attempted here due to the propagation induced differences between observations and predictions. Last, the observations discussed here indicate that there is a maximum altitude above which the aeroacoustic source becomes inefficient due to the rarefied atmosphere.

J. Acoust. Soc. Am. **139** (6), June 2016

Blom *et al.* 3137

[1]G. Kaschak, W. L. Donn, and U. Fehr, "Long-range infrasound from rockets," J. Acoust. Soc. Am. **48**(1), 12–20 (1970).

[2]N. K. Balachandran and W. L. Donn, "Characteristics of infrasonic signals from rockets," Geophys. J. Int. **26**, 135–148 (1971).

[3]N. K. Balachandran, W. L. Donn, and G. Kaschak, "On the propagation of infrasound from Rockets: Effects of Winds," J. Acoust. Soc. Am. **50**(2), 397–404 (1971).

[4]W. L. Donn, N. K. Balachandran, and D. Rind, "Tidal wind control of long-range rocket infrasound," J. Geophys. Res. **80**(12), 1662–1664, doi:10.1029/JC080i012p01662 (1975).

[5]D. O. ReVelle, "Infrasound signatures of ballistic missiles," LA-UR-02-5350, Los Alamos National Laboratory, Los Alamos, NM (2002).

[6]S. M. Tenney, J. M. Noble, R. W. Whitaker, and D. O. ReVelle, "Acoustic/infrasonic rocket engine signatures," in *AeroSense 2003* (International Society for Optics and Photonics, 2003), pp. 30–41.

[7]P. H. Rogers and J. H. Gardner, "Propagation of sonic booms in the thermosphere," J. Acoust. Soc. Am. **67**(1), 78–91 (1980).

[8]J. Olson, "Infrasound rocket signatures," in *Advanced Maui Optical and Space Surveillance Technologies Conference* (2012), Vol. 1, p. 82.

[9]A. Le Pichon, M. Garcés, E. Blanc, M. Barthélémy, and D. P. Drob, "Acoustic propagation and atmosphere characteristics derived from infrasonic waves generated by the Concorde," J. Acoust. Soc. Am. **111**(1), 629–641 (2002).

[10]M. Arrowsmith, S. Arrowsmith, and O. Marcillo, "Using sounds from the ocean to measure winds in the stratosphere," Eos **97** (2016).

[11]K. T. Walker and M. A. H. Hedlin, "A review of wind-noise reduction methodologies," in *Infrasound Monitoring for Atmospheric Studies*, edited by A. Le Pichon, E. Blanc, and A. Hauchecorne (Springer, Netherlands, 2009), pp. 141–182.

[12]P. Blom and R. Waxler, "Impulse propagation in the nocturnal boundary layer: Analysis of the geometric component," J. Acoust. Soc. Am. **131**(5), 3680–3690 (2012).

[13]D. P. Drob, J. M. Picone, and M. Garcés, "Global morphology of infrasound propagation," J. Geophys. Res. **108**(D21), 4665, doi:10.1029/2002JD003307 (2003).

[14]L. C. Sutherland and H. E. Bass, "Atmospheric absorption in the atmosphere up to 160 km," J. Acoust. Soc. Am. **115**(3), 1012–1032 (2004).

[15]M. J. Lighthill, "On sound generated aerodynamically. I. General theory," Proc. R. Soc. Lond. Ser. A **211**(1107), 564–587 (1952).